Determination of α+nucleus optical potential relevant for p-process study from the ^{nat}In(α, α) elastic scattering

Dipali Basak[1,2,*], *Tanmoy* Bar[1,2], *Lalit Kumar* Sahoo[1,2], *Sukhendu* Saha[1,2], *Tapan Kumar* Rana[3], *Chandana* Bhattacharya[3], *Santu* Manna[3], *Samir* Kundu[3], *Jayanta Kr* Sahoo[3], *Jaikiran* Meena[3], *Amiya Kr* Saha[3], and *Chinmay* Basu[1,2]

[1]Nuclear Physics Division, Saha Institute of Nuclear Physics, 1/AF, Bidhannagar, Kolkata-700064, India
[2]Homi Bhabha National Institute, Anushaktinagar, Mumbai, Maharashtra-400094, India
[3]Variable Energy Cyclotron Centre, 1/AF Bidhan Nagar, Kolkata-700064, India

Abstract. The knowledge of alpha optical potential is important for determining the nuclear reaction rates. ^{nat}In(α, α)^{nat}In elastic scttering cross-sections have been measured at energies E_{lab} = 26 and 29 MeV above the coulomb barrier. A set of local optical potential parameters was obtained from the experimental elastic scattering data. In comparison to the existing global potential parameters, the potential parameters extracted in this work show a satisfactory result. The local potential are used to calculate the ^{115}In(α, γ) reaction cross-section.

1 Introduction

The majority of heavy nuclei are synthesized in stars by neutron capture and $\beta-$decays in the s- or r-process. However, 30−35 neutron deficient nuclei (^{74}Se $-^{196}$Hg), often called p-nuclei, are produced via photo-disintegration rather than neutron capture [1–3]. In photo-disintegration process, p-nuclei are formed by the (γ,n), (γ, α) or (γ,p) reactions from s or r-seed nuclei in a high γ-flux scenario. The seed nuclei are initially moved towards the proton-rich side via a series of (γ,n) reactions. The (γ,p) and (γ, α) reactions are more rapid and produced stable elements with lower atomic number, when the neutron separation energy increases. It has been found that (γ,p) reactions are crucial for the formation of lower mass p-nuclei, whereas (γ, α) reactions produce medium and heavy masses. Due to the better availability of ion beams over γ-beams, the inverse reaction cross-sections on p-nuclei are measured and gamma induced cross-sections are extracted using the reciprocity theorem and principle detailed balance in the framework of statistical model. Statistical model calculation is sensitive to the choice of the nuclear input parameters. One of the sensitive input parameters is the entrance channel optical potential. The role of the α-optical potential is significant for the study of the (α, γ) reaction.

There are numerous global alpha optical model potentials [4, 5], but they are unable to adequately explain the (α, γ) reaction data. The ^{115}In(α, γ) reaction requires accurate knowledge of the α-optical potential at low energies. However, due to the dominance of coulomb part, the elastic scattering measurements need to be done at above barrier energies. In this study, elastic scattering angular distribution measurements of ^{nat}In(α, α) have been performed at two different energies (E = 26 and 29 MeV) above the Coulomb barrier and obtained local Wood-Saxon optical potential parameters set.

2 Experimental Setup

The experiment has been carried out at the K-130 Cyclotron facility at VECC, Kolkata. The vacuum evaporation technique was used to prepare the 99.999% chemically pure ^{nat}In targets on Al backing. By measuring the energy loss of an α-particle from a known 3-line α-source (^{239}Pu, ^{241}Am, ^{244}Cm), the thickness of the target was determined. The thickness of indium was measured to be around 66 μg/cm^2, which is approximately equivalent to 3.32×10^{17} atoms/cm^2 and roughly 730 μg/cm^2 for aluminum backing. The uncertainty of the target thickness is about 6−7%. The experimental setup is shown in Fig. 1. Elastic scattering data between θ = 23°−140° angular range was measured at two different energies (E = 26 and 29 MeV) above the Coulomb barrier. In this experiment, the cross-section was measured at a forward angle using four silicon surface barriers (SSB) ΔE-E telescopes and at a backward angle using a 16 channel silicon strip ΔE-E telescope. SSB detectors used as ΔE have a thickness of 150 μm, whereas detectors used as E have a thickness ranging from 500 to 3000 μm. The detectors used as ΔE and E, respectively, for strip telescopes have thicknesses of 52 μm and 1034 μm. A 10^0 angle of separation between each of the SSB telescopes, which were positioned on the upper turntable. There is 1^0 angular separation between each strip of a strip telescope mounted on the lower turntable. Approximately 4 mm diameter circular slits were used as collimators for the SSB telescope. The collimated area of each strip is 6×3 mm^2. Solid angles are 2.80×10^{-4} sr for SSB telescopes and 5.21×10^{-4} sr

*e-mail: dipali.basak@saha.ac.in

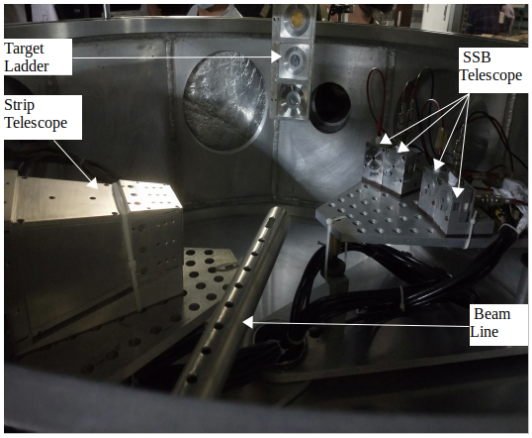

Figure 1. Experimental setup for elastic scattering

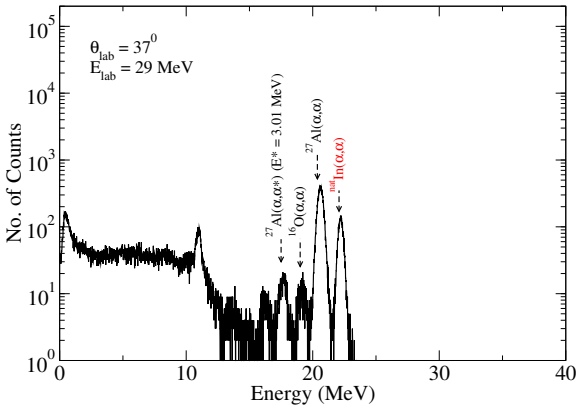

Figure 2. Energy Spectra for ^{nat}In(α,α) reaction at 29 MeV

for strip telescopes. Beam current varies between 10−15 nA during the experiment.

3 Data Analysis and Results

Fig. 2 depicts the energy spectrum of a scattered α-particle at 37° angle at a beam energy of 29 MeV. Based on the total count rate of the scattered α-particle from the target nucleus at a particular angle, the differential cross-section for that angle was calculated using the given equation,

$$\frac{d\sigma}{d\Omega} = \frac{A(\theta)}{NI\Omega} \tag{1}$$

Where I is equal to the total number of α-particle bombarding the target nucleus per unit time and N be surface density of the target material. Ω is the solid angle that the scattered particle can be detected by the detector.

The energy of the surface barrier telescopes and strip telescope has been calibrated using the known ^{229}Th α-source (4.9, 5.8, 6.3, 7.1, and 8.4 MeV) and the α-peak obtained from the ^{197}Au(α,α) scattering at E_{lab} = 26, 29, 32, and 40 MeV. The measured differential cross-sections are normalised using the theoretical Rutherford cross-sections calculated from Ref.[6]. Fig. 3 displays the experimental normalized elastic scattering cross-section at two energies.

Complex optical model potential in combination of Coulomb potential (V_c) and Nuclear potential (V_N) is given by

$$U(r) = V_c(r) + V_N(r) \tag{2}$$

Coulomb potential V_c(r) is calculated from the uniformly charged shpere of radius R_c ($R_c = r_c(A_t^{1/3} + A_t^{1/3})$) Nuclear potential consists of real (V(r)) and imaginary part (W(r)). The volume wood saxon potential is used to parameterize the real part of the nuclear potential, while the surface and volume wood saxon potentials have been taken into account for the imaginary part.

$$V(r) = V_0 f_v(r)$$

$$W(r) = \left(W_0 f_w(r) + W_s \frac{df_s}{dr}\right)$$

Volume real, volume imaginary, and surface imaginary potential depths are represented by the V_0 ,W_0 , W_s, respectively. Wood Saxon form factor is given by

$$f_i(r) = \frac{1}{1 + exp\frac{r-R_i}{a_i}} \tag{3}$$

Where

$$R_i = r_i(A_t^{1/3} + A_t^{1/3}) \qquad i = v, w, s$$

By using the search code SFRESCO[7] to fit the angular distribution of normalized differential cross-section data, a new set of potential parameters was obtained. The local potential parameters with reduced χ^2 values are listed in Table. 1 and fittings are shown by red solid line in Fig. 3

Elastic scattering cross-sections were computed using the widely used global optical potential McFadden-Satchler and Avrigeanu with the code FRESCO [7] and compared to the experimental results.

4 Discussion

In this study, normalised elastic scattering cross-section data have been fitted and local optical potential parameters were obtained at two energies E = 26 and 29 MeV. The experimental elastic scattering angular distribution data cannot be adequately explained by the two available global α-optical potentials in this energy range. A suitable local optical potenital is needed to explain the obtained experimental cross section.

The local optical potential has a real volume part and uses both volume and surface terms for the imaginary part. The spin-orbit term needs to be included in the potential form because indium has a non−zero spin parity ($\frac{9}{2}^+$). However, in Ref. [8] it has been shown that for this system, the spin-orbit impact is minimal. The local optical model potential parameters obtained from elastic scattering are extrapolated to lower energy and used in the calculation of ^{115}In(α,γ) reaction cross section using TALYS

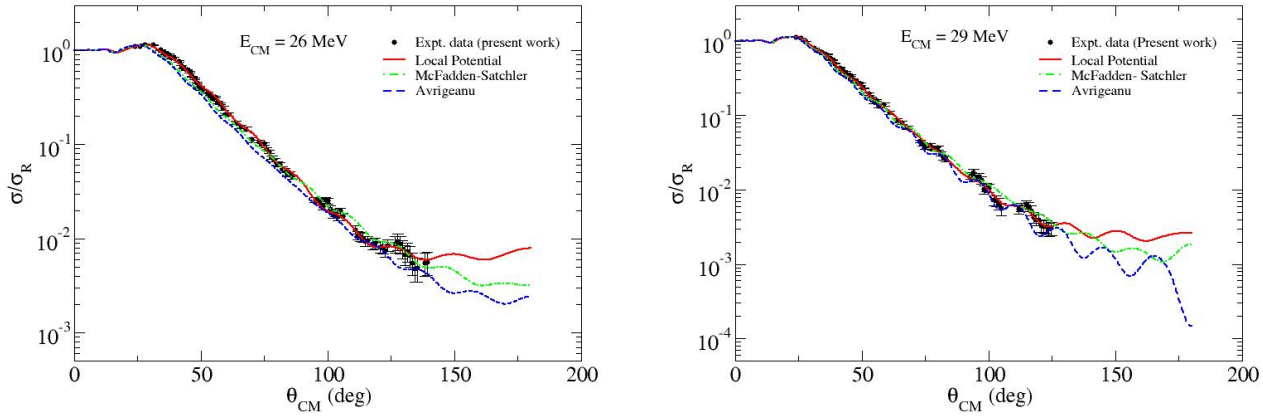

Figure 3. Experimental elasic scattering cross-section at E_{lab} = 26, 29 MeV. Theroretical calculations have been done with different global α-optical potential

Table 1. Local optical potential parameters set

E_{lab}	Volume real			Volume imaginary			Surface imaginary			χ^2/N
(MeV)	V_0	r_v	a_v	W_v	r_w	a_w	W_s	r_s	a_s	
26	49.01	1.11	0.53	8.07	1.16	0.42	13.99	1.11	0.22	1.8
29	46.35	1.15	0.53	10.02	1.16	0.42	9.99	1.15	0.26	2.4

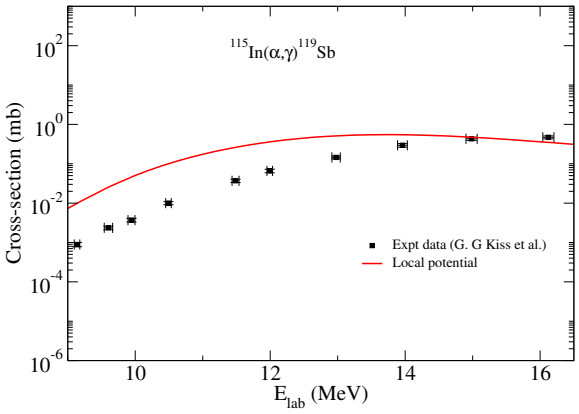

Figure 4. ^{115}In(α,γ) reaction cross-section. Exerimental reaction cross-section data from [10] compared to the theoretical predictions using local optical potential

code [9]. The local α-omp from the present elastic scattering measurement satisfactorily explain the experimental ^{115}In(α,γ) [10] excitation function mainly at higher energies and overestimated at lower energies, as shown in Fig 4. The (γ,α) cross-sections producing ^{115}In p-nucleus can then be determined using principle of detailed balance. Future plan of this work is to compare the (γ,α) rates with available abundance data.

Acknowledgments

Author would like to thank the VECC cyclotron facility for their help during the experiment. Author also acknowledges FRENA target facility for preparation of enriched indium target.

References

[1] S.E. Woosley and W.M.Howard, ApJS **36**, (1978) 285.
[2] M. Rayet et al., Astron. Asrophys. **227**, (1990) 271.
[3] M. Arnould, S. Goriely, Physics Reports **384**, (2003) 1-84.
[4] L. McFadden, G.R. Satchler, Nuclear Physics **84**, (1966) 177
[5] V. Avrigeanu et al., Physical Review C **90**,(2014) 044612
[6] O.B. Tarasov et al., Nuclear Physics A **701**,(2002) 661-665
[7] I.J. Thompson, Computer Physics Reports **7**,(1988) 167 - 212
[8] Dipali Basak , Chinmay Basu, International Journal of Modern Physics E **28**,(2019) 1950090
[9] A.J. Koning, S. Hilaire, S. Goriely, European Physics Journal A **59**,(2023) 131
[10] G. G. Kiss et al., Physical Review C **97**,(2018) 055803